International Journal of GEOMATE, May, 2025 Vol.28, Issue 129, pp.21-29
ISSN: 2186-2982 (P), 2186-2990 (O), Japan, DOI: https://doi.org/10.21660/2025.129.4522
Geotechnique, Construction Materials and Environment

UNCONSOLIDATED UNDRAINED SHEAR STRENGTH BEHAVIOUR: BEAUFORT'S PEAT SOILS

Mohd Syeddre Sutarno[1], Habib Musa Mohamad[1*], and Muhammad Aniq Azraei Suradi[1]

[1]Faculty of Engineering, University Malaysia Sabah, Malaysia

*Corresponding Author, Received: 17 April 2024, Revised: 03 Feb. 2025, Accepted: 09 Feb. 2025

ABSTRACT: Peat soil is a highly organic surface layer primarily derived from plant remains. Peat, on the other hand, refers to the subsurface layer of wetland systems, consisting of unconsolidated superficial layers with a high content of non-crystalline colloids (humus). It is generally dark brown to black in color, has an organic odor, and exhibits a spongy consistency. Peat soil is commonly found in swamp areas and is a partially decomposed organic layer of soil formed from plant matter that accumulates under conditions of waterlogging, high acidity, oxygen scarcity, and nutrient deficiency. Peat soils typically have a low shear strength ranging from 5 to 20 kPa, high compressibility values between 0.9 and 1.5, and a high moisture content exceeding 100%. Additionally, peat exhibits significant deformation, variable magnitudes, and specific structural characteristics, with an organic matter content exceeding 75%. The investigation of peat soil involves Unconsolidated Undrained Triaxial Tests, where parameters are studied under varying effective stresses of 13 kPa, 25 kPa, 50 kPa, and 100 kPa. Samples were collected from three different locations: Kpt-L1, Kpt-L2, and Kpt-L3. The findings indicate that peat soils from different locations yield varying results due to differences in composition. The Unconsolidated Undrained Triaxial Test was conducted on peat soil from Sabah for the first time by a researcher at the Klias Peat Swamp Field Centre in Beaufort, Sabah. Due to the high moisture content of peat soil, the Unconsolidated Undrained and Consolidated Undrained tests are not significantly different in their results.

Keywords: Consolidated Undrained, Effective Stress, Peat, Triaxial Test, Unconsolidated Undrained.

1. INTRODUCTION

Peat soils are found in all regions of the world, although they are more prevalent in the temperate and frigid zones of the Northern Hemisphere [15]. Table 1 presents the regions covered by peatlands. North America has the largest area of peat soils, covering 117.8 million hectares (M ha), followed by Europe with 75.0 M ha. Asia and the Far East have 23.5 M ha, Africa 12.2 M ha, Latin America 7.4 M ha, and Australia 4.1 M ha. Recent research by Gumbricht [4] identified a total of 1,689,171 km² in tropical peatland zones. In insular Southeast Asia (including the Indonesian portion of New Guinea), forest cover is declining at an annual rate of 1.0%. Among forest types, peat swamp forests have experienced the highest deforestation rates, with an average annual reduction of 2.2%. These forests are primarily being converted into secondary vegetation and plantations. In Malaysia, approximately 2.5 million hectares (7.74% of the total land area) are covered by peat soils [17]. Figure 1 illustrates the distribution of peat soils in Malaysia. According to Sapar [6], Sarawak accounts for 1,645,585 hectares (64.27%) of Malaysia's peat soils, while Peninsular Malaysia contains 714,156 hectares (27.89%). Sabah has the smallest peat soil coverage, with 200,600 hectares (7.83%). These peat deposits in Sabah are primarily located along the coastal areas, particularly in the Klias Peninsula and the Kinabatangan-Segama Valley. The "Sabah Peat Soil Information from an Engineering Perspective" project was established in 2016, as reported by Adnan Zainorabidin & Habib [2].

Table 1. Region covered by Peatlands.

Regions	Area (ha)
Africa	12.2 M
Latin America	7.4 M
Asia and the Far east	23.5 M
Australia	4.1 M
North America	117.8 M
Europe	75.0 M
Total	240 M

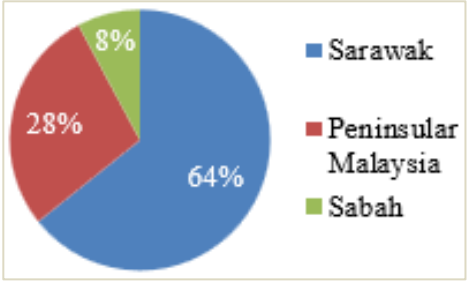

Fig.1 Percentage Peat Soil in Malaysia

The Triaxial Shear Test is commonly used to evaluate the mechanical characteristics of various deformable solids, particularly materials such as soil (e.g., sand and clay), rock, and other granular substances or powders. This testing method includes several variations, namely the Unconsolidated Undrained (UU), Consolidated Undrained (CU), and Consolidated Drained (CD) triaxial tests. This research focuses exclusively on conducting the UU test, as the objective is to obtain results that closely resemble the on-site conditions of peat soil. Peat soil at the depth of the sampled layers remains unconsolidated, and consolidation would not occur. Additionally, due to its high organic content, peat tends to retain significant moisture, making the undrained condition more representative of its natural state.

The UU test is characterized by the rapid application of loads, during which the sample is not allowed to consolidate. The sample is subjected to effective stress at a constant rate [8]. The primary objective of this study is to investigate the shear strength of Beaufort's peat soils using the Unconsolidated Undrained Triaxial Test. Furthermore, this research aims to generate a new dataset that can be utilized in future studies, particularly to enhance the understanding of Beaufort's peat soils.

Fig.2 Triaxial Test – Unconsolidated Undrained Set Up

2. RESEARCH SIGNIFICANCE

The Unconsolidated Undrained Triaxial Test was conducted to analyze the condition of peat soils, providing valuable data for future research and development. This test was specifically applied to peat soil in Sabah, representing a significant milestone as it was the first time the test was performed by a researcher at the Klias Peat Swamp Field Centre in Beaufort, Sabah. The results from this test are expected to play a crucial role in advancing our understanding of peat soil behavior and improving construction practices in similar environments.

3. MATERIAL

The Unconsolidated Undrained Triaxial Test is a widely used method in geotechnical engineering for evaluating the shear strength of soils, including peat soil. This test examines the undrained stress-strain behaviour of a cylindrical soil specimen subjected to triaxial compression loading without prior consolidation. By performing the test under various confining pressures, it provides critical parameters for undrained shear strength. This method is versatile and applicable to all types of soils.

4. METHODS

According to ASTM D2850-23 [13], the procedure can be broken down into five parts. First, a representative sample of peat soil is collected using a peat sampler (50 mm in diameter and 100 mm in height). Soil collected via this method is referred to as an undisturbed soil sample, as it better reflects the soil structure at the site compared to remolded samples. Shear strength tests should always be conducted on undisturbed soil samples for greater accuracy. Next, the undisturbed soil sample is placed into the triaxial chamber after being carefully wrapped with a membrane and secured with O-rings. The triaxial chamber is a device used to apply confining pressure to the soil specimen. Then, effective pressures of 13 kPa, 25 kPa, 50 kPa, and 100 kPa are applied by introducing cell pressure around the specimen in the triaxial chamber. These values are selected to simulate real-world conditions, replicating the typical field stresses that soils may experience. This ensures the findings are relevant to practical geotechnical engineering applications, where understanding soil behavior under various stress conditions is crucial for designing stable and safe structures. During the test, the drainage valve remains closed to prevent specimen consolidation. After applying the confining pressure, the specimen is subjected to shearing by applying a constant undrained compression loading rate of 0.1 mm/min [16]. At this stage, only the total stresses are controlled and recorded, and the test runs for up to three hours for each effective pressure. Finally, the applied stresses, axial strain, and pore water pressure are recorded during the test, and these measurements are used to calculate the shear strength of the soil.

5. DATA ANALYSIS

In this heading will be discussed on the comparison of the result for three different locations of sample in Klias Peat, Beaufort, Sabah. In named as Kpt-L1, Kpt-L2, and Kpt-L3.

5.1 Deviator Stress (kPa) vs Axial Strain (%)

The graph in Figure 3 illustrates the relationship between Deviator Stress (kPa) and Axial Strain (%), specifically for Kpt-L1. Overall, the graphs exhibit an upward trend, with each graph reaching its own maximum failure limit in terms of Deviator Stress (kPa) and Axial Strain (%). This suggests that an increase in Effective Stress leads to a higher stress-strain rate, in line with the associated stress-strain relationship. This finding is consistent with the work of Cola and Cortezolla (2005) [3]. The 100kPa Effective Stress produced the highest Deviator Stress among the other loads, with a value of 374.62kPa and an Axial Strain of 20.70%, even though the graph initially starts at a lower value due to compression forces during sample preparation prior to testing. The 50kPa Effective Stress produced the second-highest Deviator Stress at 294.84kPa, with an Axial Strain of 20.00%, followed by the 25kPa and 13kPa Effective Stresses in the Kpt-L1 graph. The Deviator Stress at 100kPa Effective Stress in Klias Beaufort, Sabah (Kpt-L1) was the highest when compared to a previous study conducted in Bukau Api-Api, Sabah, which recorded only 92.03kPa [12]. Based on the graph in Figure 3, it can be concluded that the 13kPa Effective Stress resulted in the lowest Deviator Stress and Axial Strain for Kpt-L1.

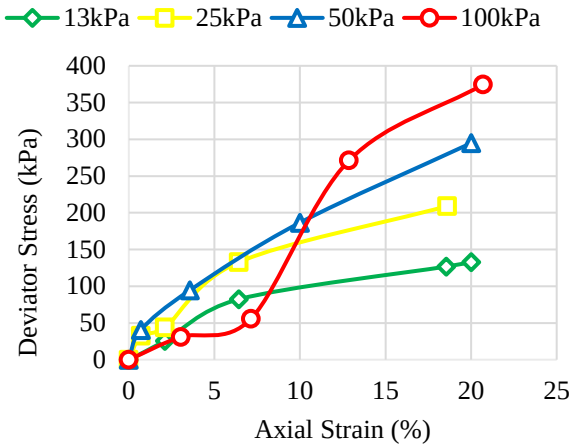

Fig.3 The Kpt-L1 Graph of Deviator Stress (kPa) to Axial Strain (%)

The graph in Figure 4 shows the relationship between Deviator Stress (kPa) and Axial Strain (%) for Kpt-L2, which also displays an upward trend. Each graph reaches its own maximum failure limit for Deviator Stress (kPa) and Axial Strain (%). The 100kPa Effective Stress generated the highest Deviator Stress, with a value of 131.45kPa. However, for Axial Strain (%), the 13kPa Effective Stress produced the highest value at 20%, compared to the others, where the Axial Strain was 18.9% for the 100kPa Effective Stress. Both the 50kPa and 13kPa Effective Stresses resulted in an Axial Strain of 19.3%, as seen in the graph for Kpt-L2. Notably, the shear strength of the Kpt-L2 sample degraded during the static load, as evidenced by the increasing triaxial test under unconsolidated undrained conditions with a movement rate of 0.01mm/min. The Axial Strain percentage of 19.3% at 13kPa Effective Stress in Kpt-L2 was similar to the values observed in Parit Nipah and Penor, which showed an Axial Strain of 20%, as found by Adnan and Habib [14]. These results support the idea that higher Deviator Stress (kPa) does not necessarily correlate with higher Axial Strain (%). The graph also indicates that Kpt-L1 and Kpt-L3 have lower initial tangents compared to Kpt-L2, likely due to differences in peat soil density. Denser soils tend to have particles that are more tightly packed, leading to greater interparticle friction and resistance to deformation. This observation is consistent with the behavior seen during soil sampling.

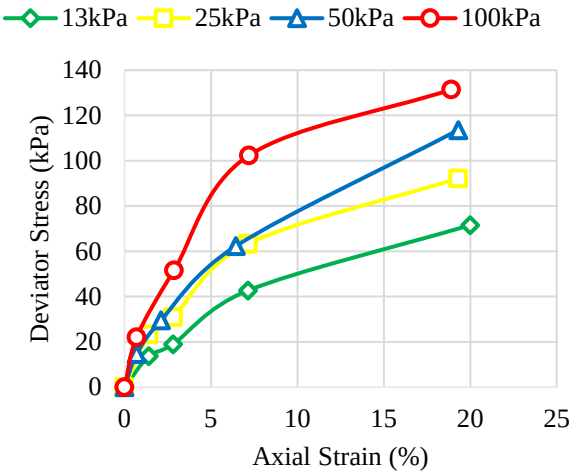

Fig.4 The Kpt-L2 Graph of Deviator Stress (kPa) to Axial Strain (%)

In the analysis of Kpt-L3 (Figure 5), it was found that Parit Nipah peat exhibits varying Deviator Stress values depending on the Effective Stress and Axial Strain. The 100kPa Effective Stress resulted in the highest Deviator Stress, while the 13kPa Effective Stress produced the lowest Deviator Stress at approximately 106.8kPa with an Axial Strain of 20%. The Kpt-L3 results show that the Deviator Stress at 13kPa Effective Stress (106.8kPa) is greater than that at 100kPa Effective Stress for Parit Nipah peat

(90kPa) [12]. The trend in Figure 5 also shows an upward trajectory, indicating that each Effective Stress reaches its maximum failure limit before decreasing during testing. The composition of the peat plays a significant role in the Deviator Stress results, with Kpt-L3 peat being more compact during sampling, possibly due to the forecasted sunny weather. Various factors such as the magnitude of applied load, soil composition, past stress history, void ratio, and the method of stress application can all influence strain magnitude in soil, as noted by Anggraini [1]. Higher moisture content and decomposition typically result in lower shear strength, while higher mineral content increases shear strength, as discussed by Munro [5]. Fibrous peat has an open structure with interstices filled by a secondary arrangement of fine, non-woody fibrous elements [9]. Additionally, the depth of the peat also plays a significant role in determining its shear strength. In conclusion, the Deviator Stress of peat soil varies depending on the area of study and the condition of the soil.

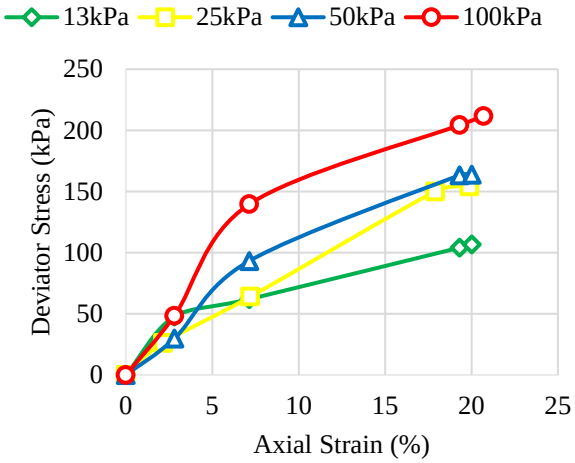

Fig.5 The Kpt-L3 Graph of Deviator Stress (kPa) to Axial Strain (%)

5.2 Eff. Axial Stress (kPa) vs Axial Strain (%)

Figure 6 displays the results of a Triaxial Test - unconsolidated-undrained (UU) for Kpt-L1, where Eff. Axial Stress (kPa) was plotted against Axial Strain (%). The graph shows that the highest Eff. Axial Strain (kPa) was observed under 100kPa Effective Stress, followed by 50kPa, 25kPa, and 13kPa. The graph line has an upward trend, indicating that when Eff. Axial Stress (kPa) increases, Axial Strain (%) also increases. The highest Eff. Axial Stress observed was 374.6kPa, represented by the red line which corresponds to 100kPa Effective Stress. The blue line shows the 50kPa Effective Stress and has a maximum Eff. Axial Stress (kPa) of 296.57kPa with a maximum Axial Strain (%) of 20%. The yellow line represents the 25kPa Effective Stress, with an Eff. Axial Stress (kPa) of 212.1kPa and 18.6% Axial Strain. The lowest Eff. Axial Stress observed was 128.1kPa for 13kPa Effective Stress, shown by the green line. From the results in Figure 6, it can be concluded that Kpt-L1 exhibits maximum Eff. Axial Stress at every Effective Stress level, where the difference between the lines was greater than the difference between their Axial Strain (%) ranging from 18% to 20%.

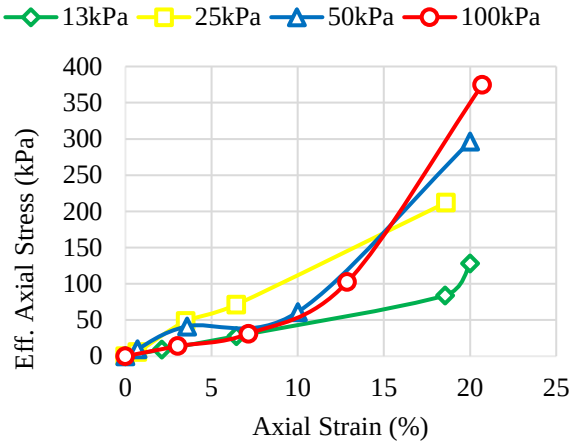

Fig.6 The Kpt-L1 Graph of Eff. Axial Stress (kPa) to Axial Strain (%)

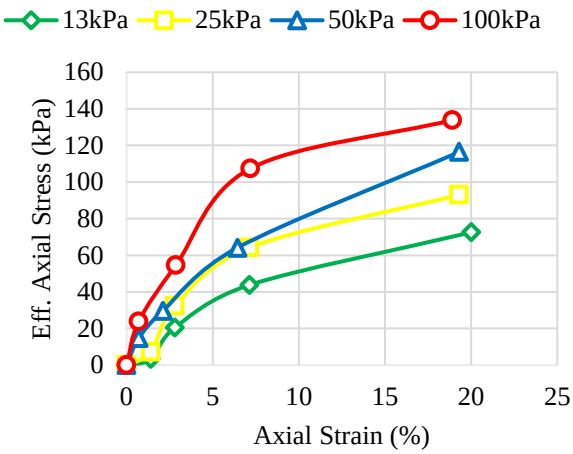

Fig.7 The Kpt-L2 Graph of Eff. Axial Stress (kPa) to Axial Strain (%)

Figure 7 depicts the relationship between Eff. Axial Stress (kPa) and Axial Strain (%) for Kpt-L2. The graph shows that the maximum Eff. Axial Stress has consistently increased by an average of 20kPa. The difference between the maximum Eff. Axial Stress of the yellow lines and the green line is 20.5kPa, with the green line plotted at 72.2kPa. The red line has the highest maximum Eff. Axial Stress among the four lines, with a value of 133.82kPa, which is greater than the blue line's maximum of 116.44kPa. During testing, it was observed that the higher the Effective Stress applied, the shorter the

body of the sample as shown in Figure 9, which could be related to the bulging condition of the sample. The Axial Strain of Kpt-L2 indicates that the range for the Axial Strain that underwent Triaxial Test - unconsolidated-undrained (UU) is 18-20%, which is the same as the Axial Strain in a previous study in Triaxial Test - consolidated-undrained (CU) conducted at Kitamura Peat and Namporo Peat, Japan [7]. In conclusion, the graph shows that the greater the Effective Stress applied to peat soil, the greater the Eff. Axial Stress.

The graph in Figure 8 displays the relationship between Eff. Axial Stress (kPa) and Axial Strain (%). The graph shows that the lowest Eff. Axial Stress (kPa) was observed at 13kPa Effective Stress, and the highest was seen at 100kPa Effective Stress.

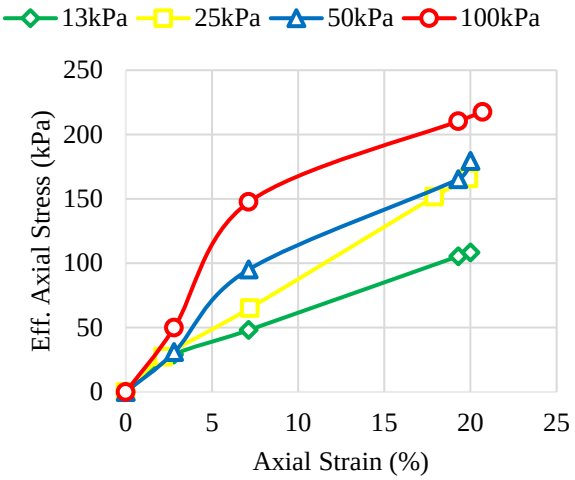

Fig.8 The Kpt-L3 Graph of Eff. Axial Stress (kPa) to Axial Strain (%)

Fig.9 The Peat Soil Sample After Testing

The second highest was at 50kPa, followed by 25kPa. The graph demonstrates that as Effective Stress (kPa) increases, Axial Strain (%) and Eff. Axial Stress (kPa) also increase. The highest Eff. Axial Stress observed was 217.56kPa, which is lower than the Eff. Axial Stress plotted in Kpt-L1, which is 374.6kPa, represented by the red line corresponding to 100kPa Effective Stress in Fig.6. The blue line represents 50kPa Effective Stress and has a maximum Eff. Axial Stress (kPa) of 108.25kPa with a maximum Axial Strain (%) of 20%. The yellow line represents the 25kPa Effective Stress, with an Eff. Axial Stress (kPa) of 165kPa. The green line shows the lowest Eff. Axial Stress observed at 128.1kPa for 13kPa Effective Stress. From the results in Figure 8, the highest Effective Axial Strain in Kpt-L3 was 217.56kPa, which is lower than Kpt-L1's 100kPa Effective Stress, which had an Eff. Axial Stress of 374.6kPa. It can be concluded that different location samples will produce different results even if the Effective Stress applied is the same.

5.3 Shear Strain (%) vs Axial Strain (%)

Figure 10 shows the results of a Triaxial Test - unconsolidated-undrained (UU) for Kpt-L1. The graph plots Shear Strain (%) against Axial Strain (%). The results indicate that the maximum Shear Strain (%) was observed under Effective Stress of 100kPa, 50kPa, 25kPa, and 13kPa almost the same in the range of 6.0% - 6.7%. The difference in Shear Strain recorded in Kpt-L1 was not significant. The minimum Shear Strain was observed due to the similar actual condition of the sample during testing, where the movement of the direction of the body sample was minimal compared with the original condition. The graph shows an upward movement of Shear Strain (%) same as to Axial Strain (%). Axial Strain for each line hit the maximum in average 20%, even though different Effective Stress was applied. Based on the results, it can be concluded that the movement of Shear Strain in Kpt-L1 is minimal.

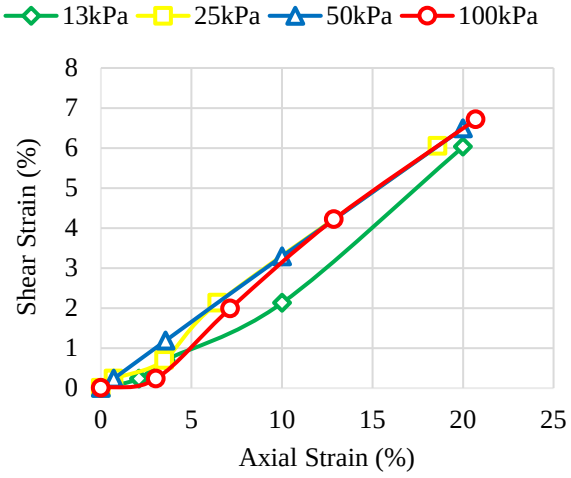

Fig.10 The Kpt-L1 Graph of Shear Strain (%) to

Axial Strain (%)

Based on the data presented in Figure 11, we can see the relationship between Shear Strain (%) and Axial Strain (%) of Kpt-L2. The graph is non-linear, indicating that the motion is non-uniform. The slope of the graph decreases with increasing Axial Strain (%). The graph shows a sudden jump in the first four points, followed by a slower increase until it reaches the maximum Shear Strain of 5.9% to 6.9% at 13kPa, 25kPa, 50kPa, and 100kPa. The behaviour of the sample during testing also supports this observation, as the movement of the sample changes drastically at the beginning of testing and becomes slow towards the end until it reaches the maximum Shear Strain. The sample's bottom layer appears to be more tender compared to the top layer, which is stiffer. These results suggest that the different layers within the sample can lead to a non-uniform motion of the graph, as shown in Fig.11.

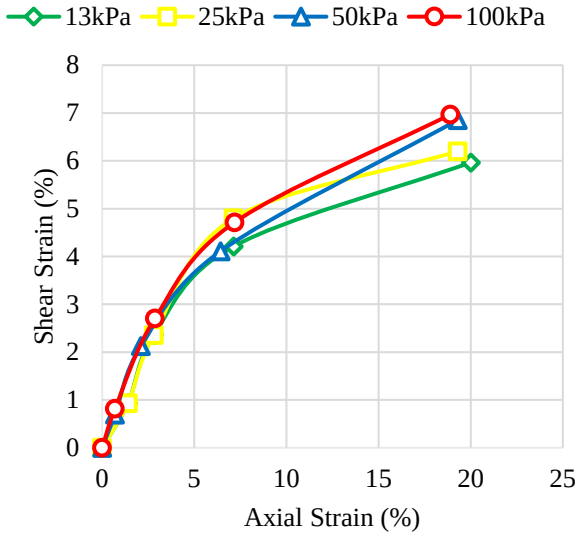

Fig.11 The Kpt-L2 Graph of Shear Strain (%) to Axial Strain (%)

In Figure 12, the results of a Kpt-L3 are displayed. The graph shows the relationship between Shear Strain (%) and Axial Strain (%) for different Effective Stresses (100kPa, 50kPa, 25kPa, and 13kPa). It is observed that Shear Strain (%) and Axial Strain (%) are directly proportional to each other for all Effective Stresses. The graph shows that each Effective Stress applied produces similar results. Peat often exhibits anisotropic behaviour due to its fibrous structure [10]. The direction of fibres and the degree of decomposition significantly influence the stress-strain response. In the case of Kpt-L3, the orientation of fibres is more consistent across samples compared to Kpt-L2 and Kpt-L1, leading to overlapping graph results despite the application of various effective stress levels. This consistency in fibre orientation results in a more uniform stress-strain response for Kpt-L3, whereas the variability in fibre orientation and decomposition degree in Kpt-L2 and Kpt-L1 contributes to the differences observed in their respective stress-strain graphs. The maximum Shear Strain for the green line is 6.4% with an Axial Stress of 20%. For the yellow line, the Shear Strain is 6.4% and the Axial Strain is 19.9%. For the blue line, the Shear Strain is 6.4% and the Axial Strain is 20%. Finally, for the red line, the Shear Strain is 6.7% and the Axial Strain is 20.7%. Based on these results, the maximum average for Shear Strain in Kpt-L3 is 20.15%, and for Axial Strain, it is 6.5%. Overall, the results indicate that the Kpt-L3 is not affected by Effective Stress. Even when the Effective Stress increases, the outcome remains almost the same.

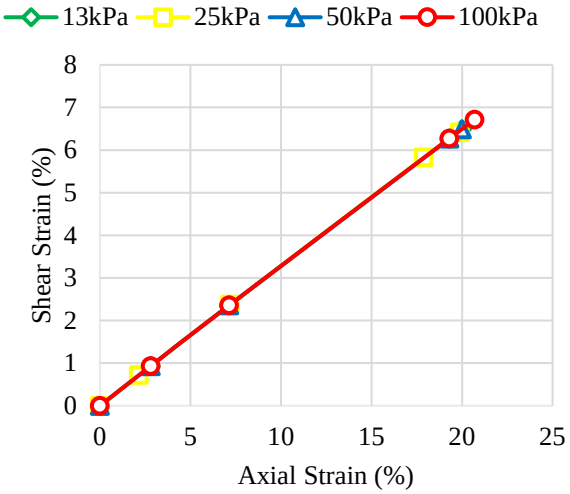

Fig.12 The Kpt-L3 Graph of Shear Strain (%) to Axial Strain (%)

5.4 Axial Stress (kPa) to Axial Strain (%)

Figure 13 illustrates the results of a Triaxial Test - unconsolidated-undrained (UU) conducted on Kpt-L1. The graph depicts Axial Stress (kPa) plotted against Axial Strain (%). The data indicates that the highest

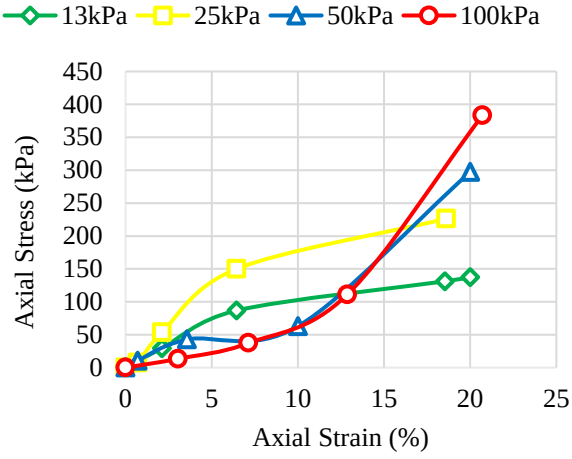

Fig.13 The Kpt-L1 Graph of Axial Stress (kPa) to

Axial Strain (%)

Axial Strain (kPa) was observed under 100kPa Effective Stress, followed by 50kPa, 25kPa, and 13kPa. The upward trend of the graph signifies that as Axial Stress (kPa) increases, Axial Strain (%) also increases. The highest recorded Axial Stress was 383.3kPa with an Axial Strain of 20.7%, represented by the red line corresponding to 100kPa Effective Stress. Similarly, the blue line represents 50kPa Effective Stress, reaching a maximum Axial Stress of 297.4kPa and maximum Axial Strain (%) of 20%. Both the red and blue lines show a gradual increase in slope from the beginning of the graph until reaching a maximum Axial Strain. Conversely, the yellow and green lines demonstrate a decrease in slope as Axial Strain (%) increases until reaching the maximum Axial Stress. During testing, it was observed that changes in the length of the sample body were significantly slower under 100kPa and 50kPa effective stress compared to 25kPa and 13kPa. The latter exhibited a drastic change in body length at the beginning of testing. This behaviour is attributed to the high-water content and low permeability of peat soil [11]. When an axial load is applied, pore water pressure may increase rapidly. If the pore pressure increases faster than it can dissipate, the effective stress initially decreases, leading to a reduction in axial stress. This phenomenon was particularly evident under the 50kPa and 100kPa effective stresses, where the changes in sample length were more gradual. Based on these results, it can be concluded that Effective Stresses of 100kPa and 50kPa exhibit the slowest changes in the initial stages of testing in Kpt-L1.

Figure 14 illustrates the relationship between Axial Stress (kPa) and Axial Strain (%) for Kpt-L2. The graph reveals a consistent increase in the maximum Axial Stress, averaging 20kPa.

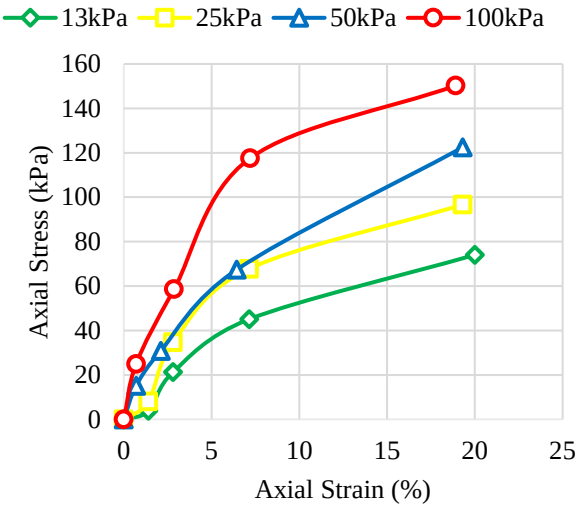

Fig.14 The Kpt-L2 Graph of Axial Stress (kPa) to Axial Strain (%)

Notably, the difference between the maximum Axial Stress of the yellow lines and the green line is 20.5kPa, with the green line plotted at a maximum axial stress of 74kPa, while the yellow line reaches a maximum of 96.64kPa. Among the four lines, the red line exhibits the highest maximum Axial Stress, recording a value of 150.23kPa, differing by 27.81kPa from the blue line's maximum of 122.42kPa. Observation during testing revealed that as the Effective Stress applied increased, the body of the sample shortened, possibly due to the bulging condition of the sample. The Axial Strain of Kpt-L2 indicates a range of 18.9% to 20% for the Axial Strain experienced during the Triaxial Test - unconsolidated-undrained (UU). In summary, the graph shows that increasing the Effective Stress applied to peat soil in Kpt-L2 leads to a greater Axial Stress.

The graph shown in Figure 15 is the relationship between Axial Stress (kPa) and Axial Strain (%). It is evident from the graph that the lowest Axial Strain (kPa) was observed at 13kPa Effective Stress, while the highest was recorded at 100kPa Effective Stress. The second highest was observed at 50kPa, followed by 25kPa.

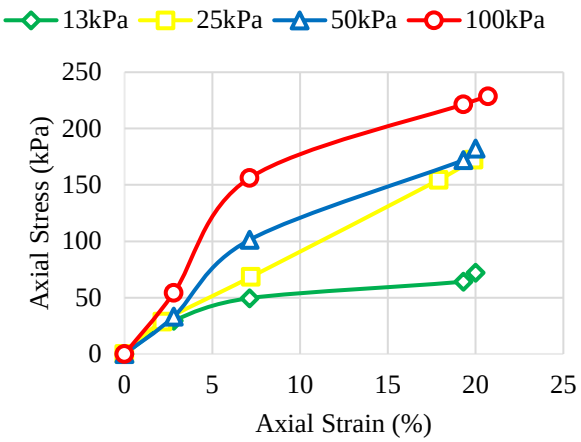

Fig.15 The Kpt-L3 Graph of Axial Stress (kPa) to Axial Strain (%)

The graph further demonstrates that as Effective Stress (kPa) increases, both Axial Strain (%) and Axial Stress (kPa) also increase. The highest Axial Stress observed in this test was 228.78kPa, which is lower than that recorded in Kpt-L1, measured at 383.3kPa, represented by the red line corresponding to 100kPa Effective Stress. The blue line, indicating 50kPa Effective Stress, reached a maximum Axial Stress (kPa) of 182.36kPa with a maximum Axial Strain (%) of 20%. The yellow line, epresenting 25kPa Effective Stress, exhibited an Axial Stress (kPa) of 172.5kPa. The graph also highlights a minimal difference between the blue and yellow lines, with only 9.86kPa separating them. This subtle difference was reflected in the sample during testing,

where the body length remained almost the same in Kpt-L3. Conversely, the green line depicted the lowest Axial Stress observed at 72.27kPa for 13kPa Effective Stress. From the results presented in Fig 4.12, it can be inferred that varying Effective Stress applied do not necessarily result in significant differences in maximum of Axial Stress.

5.5 Deviator Stress (kPa) vs Axial Strain (%)

Table 2 presents the result of the Cohesion, C and Friction Angle, Ø and Figure 16 shows the typical Mohr Circle of Deviator Stress (kPa) to Normal Stress (kPa) for the results of Kpt-L1, Kpt-L2, and Kpt-L3 after undergoing a Triaxial Test - Unconsolidated Undrained, with varying effective stress levels applied. The table details the cohesion and friction angle for each test result. Based on the Mohr Circle, Kpt-L1 recorded a cohesion of 25kPa with a friction angle of 20.84˚. Kpt-L2 exhibited a cohesion of 12kPa and a friction angle of 11.68˚, the lowest values among the three samples. Kpt-L3 recorded a cohesion of 20kPa with a friction angle of 15.25˚.

Table 2. Result of The Cohesion, C and Friction Angle, Ø

	L1		L2		L3	
Cohesion, C	25kPa		12kPa		20kPa	
Friction angle, Ø	20.84		11.68		15.25	
	Failure Envelope					
Deviator Stress (kPa)	0	197	0	150	0	165
Normal Stress (kPa)	25	100	12	43	20	65

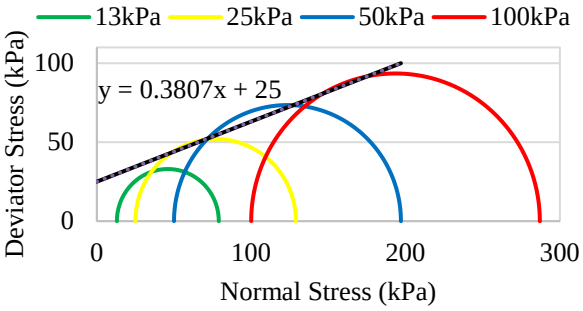

Fig.16 Typical Mohr Circle of Deviator Stress (kPa) to Normal Stress (kPa)

These results suggest variability in cohesion and friction angles due to differences in composition among the peat soil samples collected from three distinct areas. It can be concluded that peat soil generally has a higher friction angle compared to clay, which typically has a friction angle of about 5˚ [11]. This observation emphasizes the unique properties of peat soil and underscores the importance of considering composition variations in different regions when assessing cohesion and friction angle.

6. CONCLUSIONS

The objective of this research has been successfully achieved through the conducted tests and the analysis of the results. It can be concluded that different locations yield different outcomes due to variations in the composition of peat soils. When comparing the current results from Triaxial testing of Unconsolidated Undrained samples with a previous study on Consolidated Undrained samples, it can be concluded that there is no significant difference between the two tests, as the water content of the peat soil is high. This research fills a notable gap in the existing literature, as the data collected represents the first-ever dataset derived from these specific tests. This study marks the inaugural attempt by a researcher at the Klias Peat Swamp Field Centre in Beaufort, Sabah, to conduct such investigations.

7. REFERENCES

[1] Anggraini V., Shear strength improvement of peat soil due to consolidation. Master Dissertation, Universiti Teknologi Malaysia, 2006.

[2] Adnan Z. and Habib Musa M., A geotechnical exploration of Sabah peat soil: Engineering classifications and field surveys. Electronic Journal of Geotechnical Engineering. 21(20), 2016, pp. 6671–6687.

[3] Cola S. and Cortezolla G., The shear strength behaviour of two peaty soils. Geotechnical and Geological Engineering, 23, 2005, pp. 679–695.

[4] Gumbricht T., Roman-Cuesta R. M., Verchot L., Herold M., Wittmann F., Householder E., Herold N., and Murdiyarso D., An expert system model for mapping tropical wetlands and peatlands reveals South America as the largest contributor. Global Change Biology 23(9), 2017, pp. 3581–3599.

[5] Munro R., Dealing with bearing capacity problems on low volume roads constructed on peat. The Highland Council, Environmental and Community Service, HQ, Glenurquhart Road, Interness IV3 5NX Scotland, 2014.

[6] Nurul Irah Fazirah Sapar, Siti Jahara Matlan, Habib Musa Mohamad, Rohaya Alias and Aniza Ibrahim, A Study on Physical and Morphological Characteristics of Tropical Peat in Sabah, International Journal of Advanced Research in Engineering and Technology, 11(11), 2020, pp. 542-553.

[7] Nobutaka Yamazoe, Tanaka H., Ogino T., and Nishimura S., Mechanism of sampling

disturbance for peat ground and its influence on mechanical properties. Soils and Foundations, 63(5), 2023, pp. 101361–101361.

[8] Hossain S., Md Azijul Islam, Faria Fahim Badhon, and Imtiaz T., Triaxial Test. Pressbooks.pub; Mavs Open Press 2021.

[9] Hameedi M. K., Omari A., and Fattah M. Y., Compression and Creep Indices of Organic Clayey Soil. IOP Conference Series. Materials Science and Engineering, 671(1), 2020.

[10] Acharya M., Hendry M., and Martin C., Creep behaviour of intact and remoulded fibrous peat. Acta Geotechnica, 13, 2017, pp. 399-417.

[11] Basack S., and Purkayastha R., Engineering properties of marine clays from the eastern coast of India. Journal of Engineering and Technology Research, 1(6), 2009, pp. 109–114.

[12] Zainorabidin A., and Mohamad H. M., An Observation of The Undrained Shear Strength Characteristic of Bukau Api-Api Sabah and Parit Nipah Johor peat, EJGE, 2016.

[13] ASTM D2850-23. Standard Test Method for Unconsolidated-Undrained Triaxial Compression Test on Cohesive Soils. American Society for Testing and Materials, 2023.

[14] Zainorabidin A., and Mohamad H. M., Pre-and post-cyclic behavior on monotonic shear strength of Penor peat. Electronic Journal of Geotechnical Engineering, 20(16), 2015, pp. 6927-6935.

[15] Li P., Holden J., Irvine B., and Mu X., Erosion of Northern Hemisphere blanket peatlands under 21st ‑ century climate change. Geophysical Research Letters, 44, 2017, pp. 3615 - 3623.

[16] Wichtmann T. and Triantafyllidis T., An experimental database for the development, calibration and verification of constitutive models for sand with focus to cyclic loading: part I—tests with monotonic loading and stress cycles." Acta Geotechnica, 11, 2016, pp. 739-761.

[17] J. Miettinen, C. Shi and Soo Chin Liew., Land cover distribution in the peatlands of Peninsular Malaysia, Sumatra and Borneo in 2015 with changes since 1990. Global Ecology and Conservation, 6, 2016, pp. 67-78.